

solidfmm: A highly optimised library of operations on the solid harmonics for use in fast multipole methods

MATTHIAS KIRCHHART, Applied and Computational Mathematics, RWTH Aachen, Germany

We present `solidfmm`, a highly optimised C++ library for the solid harmonics as they are needed in fast multipole methods. The library provides efficient, vectorised implementations of the translation operations M2M, M2L, and L2L, and is available as free software. While asymptotically of complexity $O(P^3)$, for all practically relevant expansion orders P , the translation operators display an empirical complexity of $O(P^2)$, outperforming the naïve implementation by orders of magnitude.

CCS Concepts: • **Applied computing** → *Engineering; Astronomy; Physics*; • **Software and its engineering** → *Software libraries and repositories*; • **Mathematics of computing** → **Mathematical software performance**.

Additional Key Words and Phrases: fast multipole methods, solid harmonics, library, high-performance, vectorisation

1 INTRODUCTION

1.1 Summary

`solidfmm` is a highly optimised C++ library for operations on the solid harmonics as they are needed in fast multipole methods.

- Supports both single and double precision.
- Fully vectorised on x86 CPUs with support for AVX or AVX-512.
- Hand-written assembly implementations for maximal performance of critical parts.
- Supports mixed order translations: you can do M2M, M2L, L2L with differing input and output orders. This is important for adaptive, variable order fast multipole codes.
- Translations support arbitrary shift vectors.
- No dependence on external libraries except for the C++ standard library.
- Thread safe and exception safe.
- Lean. The library interface is very small and easy to use. We used encapsulation using handles to avoid dependence of user code on implementation details.
- Free software. Licenced under the GNU General Public License as published by the Free Software Foundation, either version 3, or, at your option, any later version.

`solidfmm` is available from the author's institution at <https://rwth-aachen.sciebo.de/s/YIJFvSERVBiOkbc>, or from GitHub.

1.2 Motivation and Background

The fast multipole method (FMM) [5] has been called one of the top ten algorithms of the 20th century [1]. It allows for approximate solutions of N -body problems, namely the evaluation of:

$$u(x_i) = \sum_{j=1}^N G(x_i, x_j) q_j \quad i = 1, \dots, N, \quad (1)$$

Author's address: Matthias Kirchhart, kirchhart@acom.rwth-aachen.de, Applied and Computational Mathematics, RWTH Aachen, Schinkelstraße 2, 52062 Aachen, Germany.

where G is the so-called kernel function, N is the number of bodies with locations $x_i \in \mathbb{R}^3$ and associated masses or charges $q_i \in \mathbb{R}$, $i = 1, \dots, N$. It is straightforward to see that a direct evaluation of this sum at all particle locations requires $O(N^2)$ arithmetic operations, making this approach infeasible for large numbers of bodies N . In contrast, the FMM computes approximations of (1) in only $O(N)$ operations, resulting in dramatic speedups, where the accuracy can be controlled by the user.

This is achieved through the use of series expansions of the underlying kernel function G . These expansions are truncated at a user-defined order P , where increasing P results in more accurate, but also more expensive computations: the hidden constant in the $O(N)$ -complexity depends on P and the type of expansion used. One of the most important kernel functions is the fundamental solution of the Poisson equation, i. e., up to a factor of $(4\pi)^{-1}$, the function $G(x, y) := |x - y|^{-1}$, $x, y \in \mathbb{R}^3$. It can be used for both gravitational as well as electrical potentials. The solid harmonics have been specifically derived with this particular kernel in mind and yield the most efficient expansions available. Expansions in their terms require only $O(P^2)$ coefficients, compared to $O(P^3)$ for Chebyshev or Cartesian Taylor expansions at the same level of accuracy. Depending on the application, common values for P lie between $P \approx 3$ for fast, low-fidelity computations and $P \approx 30$ to satisfy the highest accuracy demands. Thus, by modern standards, an individual expansion is ‘small’, and millions of such expansions can be stored in the memory of even cheap hardware.

There are two different kinds of expansions in FMMs: multipole and local expansions, also called M- and L-expansions, respectively. In the so-called M2L-translation,¹ an M-expansion around one point A is converted into an L-expansion around another point B . This operation is without doubt the most crucial element of FMMs, for large N it is required millions of times and most of the computational effort lies in this stage. The direct implementation of the M2L-translation has complexity $O(P^4)$. This number is not at all that small anymore when $P \approx 30$ and millions of such operations are necessary. For this reason, several so-called ‘fast translation’ schemes have been devised reducing this complexity to $O(P^3)$ or even $O(P^2(\log_2 P)^2)$.

On the one hand, many of the commonly available FMM software projects focus on the difficult task of creating an implementation that efficiently scales to highly parallel super-computers. Very elaborate techniques are used to minimise communication, handle load balancing, and to additionally make use of GPUs when available. On the other hand, the M2L-translation in these software packages is often implemented using simple, nested loops without further optimisation. ExaFMM [11], for example, uses the straight $O(P^4)$ implementation² and additionally uses the trigonometric functions to evaluate the solid harmonics in spherical coordinates—even though they can more easily be computed in Cartesian coordinates using only square roots and elementary arithmetic [9]. Such implementations thus leave an opportunity for improvement at the local, CPU level. For this reason we believe that even sophisticated codes like ExaFMM could directly benefit from an optimised implementation of the M2L translation.

The main reason for this situation is probably that implementing fast, efficiently vectorised translation schemes for the solid harmonics is quite challenging. To our knowledge there simply is no implementation of fast translation schemes that is free (as both in beer and in liberty) and vectorised. `soliddfmm` aims to change this situation. It provides a fully vectorised implementation of an algorithm sketched by Dehnen [3] with highly optimised routines for current x86 architectures. Inspired by the BLIS [8], the performance critical parts are reduced to a handful of isolated and small ‘microkernels’ written in assembly language and compiler intrinsics, while the main part of the library is written in platform-independent standard C++. This extensible design allows us to add support for further CPU architectures

¹Strictly speaking, the term ‘translation’ is a misnomer as it also involves a conversion. Yet, the name got stuck and is now commonly used in the context of FMMs.

²See <https://github.com/exafmm/exafmm/blob/master/kernels/laplace.h>

in the future. In addition to the M2L, the library also features accelerated implementations of the other translations in FMM: M2M and L2L. The library is intended to be used the context of the aforementioned highly-parallel FMM frameworks, such that they immediately benefit from its optimisations.

In this article we will first summarise the basics of the M2L translation. The M2M and L2L translations are very similar in nature, and while also implemented in `solidfmm`, omitted here for brevity. We then continue with a very brief review of various acceleration techniques, before describing Dehnen’s approach in greater detail. We then describe how `solidfmm` implements a slightly modified version of his algorithm and finish with benchmarks comparing `solidfmm` to the simple, naïve implementation.

2 THE M2L TRANSLATION

In this section we give a review of the M2L translation. After describing its plain, canonical formulation we give a short survey of different acceleration techniques, before describing the ideas behind the current, rotation-based approach in greater detail.

2.1 Canonical Formulation

M- and L-expansions of order P , developed around respectively $x_A, x_B \in \mathbb{R}^3$ are functions of the following shape:

$$\sum_{n=0}^{P-1} \sum_{m=-n}^n M_n^m \overline{S_n^m(x - x_A)}, \quad \sum_{n=0}^{P-1} \sum_{m=-n}^n L_n^m \overline{R_n^m(x - x_B)}. \quad (2)$$

Here, R_n^m and S_n^m are complex-valued functions, respectively called the *regular* and *singular harmonics*, as defined in the appendix. The coefficients $M_n^m \in \mathbb{C}$ are also called multipoles, whereas the $L_n^m \in \mathbb{C}$ are simply called local coefficients.

For $C \in \{L, M, R, S\}$ one always has $C_n^{-m} = (-1)^m \overline{C_n^m}$. This ensures that the sums in (2) always take real values; additionally one only needs to store the coefficients with $m \geq 0$. Further space could be saved by noting that for $m = 0$ the imaginary parts $\Im(C_n^0)$ are always vanishing. However, the memory savings from this are only marginal and come at the cost of more complicated memory layouts. For this reason, in this work, we will also store $\Im(C_n^0) = 0$.

Thus, an M- or L-expansion of order P can be stored using $P(P + 1)/2$ complex, or $P(P + 1)$ real numbers in a ‘triangular shape’ as illustrated in [Figure 1](#). Lacking a better name, we will call such a triangular arrangement of coefficients a *solid*. We thus have defined solids and harmonics.³

Given a multipole expansion with coefficients M_n^m and expansion centre x_A , the corresponding local expansion at centre x_B and with coefficients L_n^m can be computed using the M2L-translation. It comes in two flavours:

$$L_n^m = (-1)^n \sum_{k=0}^{P-n-1} \sum_{l=-k}^k \overline{M_k^l} S_{n+k}^{m+l}(x_B - x_A) \quad \text{and} \quad L_n^m = (-1)^n \sum_{k=0}^{P-1} \sum_{l=-k}^k \overline{M_k^l} S_{n+k}^{m+l}(x_B - x_A), \quad (3)$$

respectively called the ‘single height’ and ‘double height’ kernels. These expressions only differ in the number of terms: for the double height kernel we need to compute S up to order $2P - 1$, while for the single height kernel order P suffices. The single height kernel is cheaper, the double height kernel is more accurate. In its naïve implementation, the double height kernel is about six times more expensive to evaluate than the single height version [2, Footnote 5]. This should be kept in mind when comparing implementations.

³For the rest of this work, we slightly deviate from the standard mathematical nomenclature, where the functions R_n^m and S_n^m themselves are called solid harmonics. For us, the functions are called *harmonics*; a set of their values at a specific point or a set of coefficients is called *solid*.

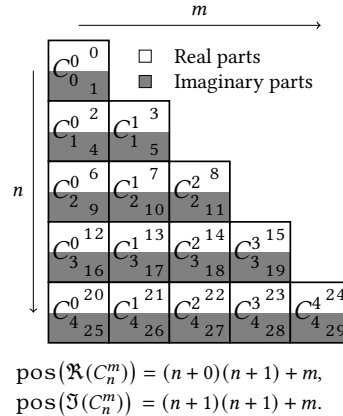


Fig. 1. The coefficients $C_n^m \in \mathbb{C}$ of both multipole and local expansions can be stored using $P(P+1)$ real numbers. In this example we have $P = 5$. They can be arranged in a triangular pattern according to their indices $n = 0, \dots, 4$ and $m = 0, \dots, n$, where the values for negative m are given implicitly by $C_n^m = (-1)^m \overline{C_n^{-m}}$. The numbers in the upper and lower right corners of the boxes denote the array position (pos) in computer memory. Throughout this work, we will refer to such an arrangement of numbers as a *solid*.

`solidfmm` implements the double height kernel, as it leads to more regular memory access patterns: every entry in L linearly depends on every entry in M . Thus, M2L can be interpreted as a linear mapping, i. e., a fully populated matrix, whose $O(P^4)$ entries $S_{n+k}^{m+l}(x_B - x_A)$ depend on the shift vector $r_{AB} := x_B - x_A$.

2.2 A Brief Survey of Fast M2L Schemes

Various approaches have been proposed to accelerate the M2L translation, a survey of the most common ones is given by Coulaud, Fortin, and Roman [2]. Some of these approaches only work when there only is a finite set of shift vector directions $r_{AB} := x_B - x_A$, which is the case in certain implementations of the FMM. These approaches include:

- BLAS-based approaches [2]. These do not break the $O(P^4)$ complexity. Instead, the finite set of translation matrices is stored explicitly, performance is achieved by using highly optimised BLAS routines to apply these matrices to many solids in parallel.
- Plane-wave expansion methods [6]. These only approximate the M2L translation and need careful tuning to match the accuracy of the original expansions for every given P .

These schemes are unsuitable for use in `solidfmm`, which aims to be flexible and permit arbitrary shifts r_{AB} and orders P . Other, more general approaches include:

- Diagonalising the translation matrix through the use of fast Fourier transforms (FFT) [4]. These approaches achieve the aforementioned complexity of $O(P^2(\log_2 P)^2)$. However, practice has shown that they suffer from numerical instabilities for $P > 16$.
- Rotation-based approaches [10]. These perform a change of coordinates, after which the translation can be carried out in $O(P^3)$ time. Finally, the result is changed back to the original coordinate system. Such changes of coordinates can also be done in $O(P^3)$ time, resulting in the same overall complexity of $O(P^3)$.

There are approaches to repair the instabilities of the FFT method, but they all come at an extra cost. Additionally, we note that $(\log_2 P)^2 \geq P$ for $4 \leq P \leq 16$, so for the stable choices of P , whether the algorithmic complexity is

favourable depends on the hidden constants and even more on the particular implementation. For these reasons `solidfmm` implements a rotation-based approach, which will be described in greater detail below.

2.3 Rotation-based Approaches

Rotation-based accelerations were introduced by White and Head-Gordon [10]. The basic idea is as follows. Assume the shift-vector r_{AB} was aligned with the z-axis, i. e., assume we had $r_{AB} = (0, 0, R)^\top$. In this case, most of the entries in the M2L-kernels (3) vanish, because:

$$S_{n+k}^{m+l}(0, 0, R) = \begin{cases} 0 & \text{if } m+l \neq 0, \\ \frac{(n+k)!}{R^{n+k+1}} & \text{if } m+l = 0. \end{cases} \quad (4)$$

We now add a minor modification, by additionally assuming that $R = 1$. Then (3) reduces to:

$$L_n^m = (-1)^{n+m} \sum_{k=m}^{P-n-1} M_k^m(n+k)! \quad \text{and} \quad L_n^m = (-1)^{n+m} \sum_{k=m}^{P-1} M_k^m(n+k)! \quad (5)$$

In other words, for $r_{AB} = (0, 0, 1)^\top$, M2L is an operation that acts *column-wise* on a solid, resulting in $O(P^3)$ complexity. Thus, for the double height kernel, the general structure of the algorithm is as follows. Given $v \in \mathbb{N}$ solids $M[0], M[1], \dots, M[v-1]$ of order P and associated shift vectors $r[0], r[1], \dots, r[v-1]$, do the following:

- (1) Perform a change of coordinates on each $M[0], \dots, M[v-1]$, such that the shift is along $(0, 0, 1)^\top$.
- (2) For each column $m = 0, \dots, P-1$, perform the following matrix–matrix product:

$$\begin{pmatrix} 2m! & (2m+1)! & (2m+2)! & \cdots & (P+m-1)! \\ (2m+1)! & (2m+2)! & (2m+3)! & \cdots & (P+m)! \\ \vdots & \vdots & \vdots & \ddots & \vdots \\ (P+m-1)! & (P+m)! & (P+m+1)! & \cdots & (2P-2)! \end{pmatrix} \begin{pmatrix} M_m^m[0] & M_m^m[1] & \cdots & M_m^m[v-1] \\ M_{m+1}^m[0] & M_{m+1}^m[1] & \cdots & M_{m+1}^m[v-1] \\ \vdots & \vdots & \ddots & \vdots \\ M_{P-1}^m[0] & M_{P-1}^m[1] & \cdots & M_{P-1}^m[v-1] \end{pmatrix}. \quad (6)$$

Note that real and imaginary parts do not couple! This matrix–matrix product can be carried out separately for real and imaginary parts. Also note that we apply the same matrix of faculties to all solids.

- (3) Apply the signs $(-1)^{n+m}$ to the results.
- (4) Reverse the change of coordinates back to the original.

Here we see why we introduced the additional assumption $R = 1$: otherwise each solid would need to be multiplied with a different matrix. Now the the matrix is constant and identical for all solids $M[0], \dots, M[v-1]$. The matrix–matrix product (6) can be highly optimised using blocking techniques from the BLIS [8] and can be carried out separately for real and imaginary parts. However, to avoid wasting precious cache space, the matrix of faculties should not be stored explicitly. It suffices to store the the values $0!, 1!, \dots, (2P-2)!$ in a vector and write a specialised routine to carry out the product (6) using this vector.

Previous authors did not carry out the scaling to $R = 1$, and left the lengths of the shift vectors r_{AB} unchanged. In this case the necessary change of coordinates corresponds to a rotation, hence the name ‘rotation-based’. We will discuss different, but equivalent methods to achieve these rotations in the following subsection.

2.4 Rotating and Scaling Coordinate Systems

While M2L along the z -axis is an operation that acts column-wise on a solid, a change of coordinates acts row-wise. Scaling is trivial: when transforming a vector as $r \mapsto sr$ for some $s > 0$, the M- und L-coefficients change as follows:

$$M_n^m \mapsto s^{n+1} M_n^m, \quad L_n^m \mapsto \frac{L_n^m}{s^n}. \quad (7)$$

The cost of this operation is negligible. Letting $s = |r|^{-1}$ the shift vector gets unit length, and it remains to perform rotations.

2.4.1 General Rotations. A general rotation takes the following form:

$$M_n^m \mapsto \sum_{l=-n}^n D_n^{l,m} M_n^l, \quad L_n^m \mapsto \sum_{l=-n}^n D_n^{m,l} L_n^l, \quad (8)$$

where the $D_n^{m,l}$ are the so-called Wigner matrices. These matrices depend on the Euler angles of the rotation in a highly non-trivial manner and its entries are very expensive to evaluate. For this, we refer to the original paper of White and Head-Gordon [10]. If, however, only a finite set of shift directions r_{AB} is permitted, these matrices can be precomputed. Again, this makes this approach unsuitable for use in `solidfmm`, which aims to allow arbitrary shift vectors r_{AB} .

2.4.2 Factorisation of the Wigner Matrix. The idea of factorising the Wigner matrices $D_n^{m,l}$ into simpler matrices goes back to Wigner himself. It has long been known that rotations around the z -axis are trivial. For any angle α , consider the transformation:

$$(x, y, z)^\top \mapsto (x \cos(\alpha) + y \sin(\alpha), -x \sin(\alpha) + y \cos(\alpha), z)^\top. \quad (9)$$

Under such rotations, the M- and L-coefficients transform as follows:

$$M_n^m \mapsto M_n^m e^{im\alpha}, \quad L_n^m \mapsto L_n^m e^{im\alpha}. \quad (10)$$

Wigner suggested precomputing the matrices $D_n^{m,l}$ for rotations by 90° around the y -axis. This way, a general rotation can be carried out by combining three trivial rotations around the z -axis with two rotations by 90° around the y -axis. In other words, we can make use of precomputed matrices $D_n^{m,l}$ for 90° , independent of the actual Euler angles of the rotation. Just like for the z -translation in (6), the same matrices $D_n^{m,l}$ are applied to all solids. The apparent drawback of this approach is that now two $O(P^3)$ operations of the shape (8) are necessary instead of just one.

2.4.3 Dehnen's Factorisation. Dehnen [3] picked up this idea in the context of M2L, and considered swapping the x - and z -axes instead. The corresponding matrices are denoted $B_n^{m,l}$, resulting in the transformations

$$M_n^m \mapsto \sum_{l=-n}^n B_n^{l,m} M_n^l, \quad L_n^m \mapsto \sum_{l=-n}^n B_n^{m,l} L_n^l. \quad (11)$$

Swapping two axes turns a right-handed coordinate system into a left-handed one. However, because this operation is carried out twice, one obtains properly oriented results in the end. This approach has several benefits:

- (1) The matrices $B_n^{m,l}$ are involutory, i. e., they are their own inverses. Afterall, swapping x and z , and then swapping them again will get you back to where you started. There thus is no need to separately store the inverses.
- (2) All entries $B_n^{m,l}$ are real-valued. Thus, real and imaginary parts decouple in (11) and can be computed separately, cutting the operation count in half.

- (3) The matrices for the real and imaginary transformations are each only 50% populated. This reduces the cost of their application again by half and will be described in more detail later.

Thus Dehnen's approach requires swapping the x- and z-axes twice, but each of these swaps only cost $O(\frac{1}{2}P^3)$ operations, making the approach competitive to precomputing the Wigner matrices $D_n^{m,l}$ for a set of fixed directions, but without the associated loss of generality.

2.4.4 Summary. In total, combining Dehnen's approach with rescaling reduces the complexity of the M2L translation from $O(P^4)$ to $O(P^3)$ by factorising the operation into:

- $O(P^3)$ operations, namely the swapping of axes and translation along $(0, 0, 1)^\top$. These operations are 'expensive', but independent of the shift vectors. These operations can thus be vectorised and highly optimised by writing them as matrix-matrix products.
- $O(P^2)$ operations, namely scaling and rotations around the z-axis. These do depend on the shift vectors, but their cost is negligible. Additionally, vectorisation of these operations is even easier than vectorisation of the matrix-matrix products.

This approach is thus ideally suited for efficient implementations modern CPUs. Dehnen mentions that he implemented a vectorised version of this scheme, but to our knowledge his code is not freely available.

3 IMPLEMENTATION

3.1 Precomputation

The precomputation stage consists of computing the matrices required for swapping co-ordinate axes and storing them in a suitable memory layout. The computation of the factorials $0!, 1!, \dots, (2P-2)!$ is trivial, and they can be stored in a simple vector. The matrices $B_n^{m,l}$ were introduced by Dehnen and we repeat his recurrence relations in the appendix. After these have been computed the corresponding matrices for the real and imaginary parts of solids can be computed. Using the facts that $M_n^m = (-1)^m \overline{M_n^{-m}}$ and $B_n^{m,l} \in \mathbb{R}$, the mappings (11) become:

$$\Re(M_n^m) \mapsto B_n^{0,m} \Re(M_n^0) + \sum_{l=1}^n (B_n^{l,m} + (-1)^l B_n^{-l,m}) \Re(M_n^l), \quad \Im(M_n^m) \mapsto \sum_{l=1}^n (B_n^{l,m} - (-1)^l B_n^{-l,m}) \Im(M_n^l), \quad (12)$$

and analogous for L_n^m . We thus define the *swap matrices* $F_n^{m,l}$ and $G_n^{m,l}$, $m, l = 0, \dots, n$ as follows:

$$F_n^{m,l} := \begin{cases} B_n^{0,m} & \text{if } l = 0, \\ B_n^{l,m} + (-1)^l B_n^{-l,m} & \text{else,} \end{cases} \quad G_n^{m,l} := \begin{cases} 0 & \text{if } l = 0 \text{ or } m = 0, \\ B_n^{l,m} - (-1)^l B_n^{-l,m} & \text{else.} \end{cases} \quad (13)$$

With this, the mappings (11) turn into:

$$\begin{aligned} \Re(M_n^m) &\mapsto \sum_{l=0}^n F_n^{m,l} \Re(M_n^l), & \Im(M_n^m) &\mapsto \sum_{l=0}^n G_n^{m,l} \Im(M_n^l), \\ \Re(L_n^m) &\mapsto \sum_{l=0}^n F_n^{l,m} \Re(L_n^l), & \Im(L_n^m) &\mapsto \sum_{l=0}^n G_n^{l,m} \Im(L_n^l). \end{aligned} \quad (14)$$

When storing the matrices $F_n^{m,l}$ and $G_n^{m,l}$, as well as when implementing the mappings (14), it is important to notice that only 50% of their entries are non-zero. In particular the matrices exhibit a checkerboard pattern, as shown in Figure 2.

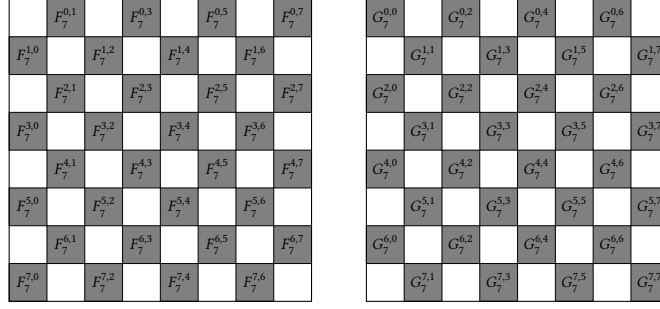


Fig. 2. The swap matrices $F_n^{m,l}$ (left) and $G_n^{m,l}$ (right), here illustrated for $n = 7$, exhibit a checkerboard pattern: every other entry is zero (white). For F_7 the pattern begins with zero, G_7 shows the opposite pattern. For even values of n the situation is reversed. Only the non-zero values should be stored to save memory and optimise the use of cache space. (More precisely, the first row and column of G_n are always entirely zero and the pattern only shows in the remaining part of the matrix. The overhead of considering these additional zeros, however, is marginal, and keeping them leads to simpler and more uniform code.)

3.2 Blocking and Packing

The computationally most expensive parts of the M2L translation consist of dense matrix–matrix products. We can thus build on the experience of the BLIS [8] developers and apply blocking techniques. In particular, when forming a matrix–matrix product $C = AB$, the matrix C is sub-divided into blocks of size $\mu \times \nu$, where the values of μ and ν are machine dependent. These blocks are then computed using the SIMD instructions of the processor, which are encapsulated in a so-called microkernel. A microkernel itself thus is machine specific, but it offers a generic, platform independent interface. The blocking scheme can thus be written using generic, platform independent code which then calls the machine specific microkernel to perform the actual computation. If necessary, A and C are padded by additional zero rows such that the total number of rows is a multiple of μ .

On many x86 systems supporting the AVX instruction set the optimal block size for double precision is $\mu = 6$ and $\nu = 8$, where B and C are stored in row-major order. On a single core of such machines, we can thus process $\nu = 8$ solids in double precision in parallel.⁴ On systems supporting AVX-512 we choose $\mu = 14$ and $\nu = 16$. Unlike the BLIS, we do not need to introduce an entire hierarchy of blocks that matches the cache hierarchy, as for realistic orders P the swap matrices F_n and G_n are comparatively small and completely fit into the L2 and L3 caches of current CPUs.

While for the product (6) the matrix A of the generic product $C = AB$ can be compressed into a single vector of faculties, for the swap matrices F_n and G_n it is stored in the so-called packed format as illustrated in Figure 3.

3.3 Buffers and Rearranging

Axis swap operations act row-wise on a solid and do not mingle real and imaginary parts. Thus, given ν solids and row n , we need to compute the products:

$$F_n \cdot \begin{pmatrix} \Re(M_n^0[0]) & \Re(M_n^0[1]) & \cdots & \Re(M_n^0[\nu-1]) \\ \Re(M_n^1[0]) & \Re(M_n^1[1]) & \cdots & \Re(M_n^1[\nu-1]) \\ \vdots & \vdots & \ddots & \vdots \\ \Re(M_n^n[0]) & \Re(M_n^n[1]) & \cdots & \Re(M_n^n[\nu-1]) \end{pmatrix}, \quad G_n \cdot \begin{pmatrix} \Im(M_n^0[0]) & \Im(M_n^0[1]) & \cdots & \Im(M_n^0[\nu-1]) \\ \Im(M_n^1[0]) & \Im(M_n^1[1]) & \cdots & \Im(M_n^1[\nu-1]) \\ \vdots & \vdots & \ddots & \vdots \\ \Im(M_n^n[0]) & \Im(M_n^n[1]) & \cdots & \Im(M_n^n[\nu-1]) \end{pmatrix}. \quad (15)$$

⁴An AVX register can only hold four double precision values. However, most Intel microarchitectures since Haswell can simultaneously execute arithmetic instructions on two such registers in a single clock cycle, giving eight values in total.

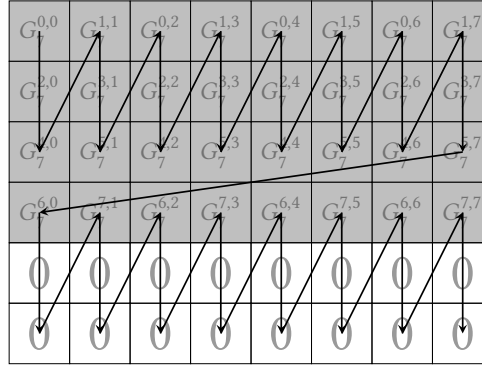


Fig. 3. On a system with $\mu = 6$, the matrix G_7 would be stored in memory as shown above. First, G_7 would be padded by with additional zero rows, such that the total number of rows is a multiple of μ . In this case four rows of zeros are padded, resulting in $G_{7,\text{padded}} \in \mathbb{R}^{12 \times 8}$. Then the first μ rows are stored in column-major order, omitting the zeros from the chequerboard pattern. The next μ rows follow, again omitting zeros according to the chequerboard pattern. When computing a matrix–matrix product with G_7 , the entries $G_7^{m,l}$ are accessed in the exact same order. We thus benefit from hardware prefetching and decreasing L1 cache misses. This technique is known as ‘packing’ [7, Section 3.3]. This requires that G_n and F_n and their respective transposes G_n^\top and F_n^\top are each packed and stored separately.

In practice these matrices of real and imaginary parts will need to be stored in row-major order and padded with zero rows, such that the total number of rows is a multiple of μ . We thus need two buffers for holding these matrices, which are then filled with data from solids that may lie scattered in arbitrary positions in memory. We will call these the swap buffers.

On the other hand, the z-translation acts column-wise on a solid. In order to carry it out efficiently, we need to store the matrices:

$$\begin{pmatrix} \Re(M_m^m[0]) & \Re(M_m^m[1]) & \cdots & \Re(M_m^m[v-1]) \\ \Re(M_{m+1}^m[0]) & \Re(M_{m+1}^m[1]) & \cdots & \Re(M_{m+1}^m[v-1]) \\ \vdots & \vdots & \ddots & \vdots \\ \Re(M_{p-1}^m[0]) & \Re(M_{p-1}^m[1]) & \cdots & \Re(M_{p-1}^m[v-1]) \end{pmatrix}, \quad \begin{pmatrix} \Im(M_m^m[0]) & \Im(M_m^m[1]) & \cdots & \Im(M_m^m[v-1]) \\ \Im(M_{m+1}^m[0]) & \Im(M_{m+1}^m[1]) & \cdots & \Im(M_{m+1}^m[v-1]) \\ \vdots & \vdots & \ddots & \vdots \\ \Im(M_{p-1}^m[0]) & \Im(M_{p-1}^m[1]) & \cdots & \Im(M_{p-1}^m[v-1]) \end{pmatrix}, \quad (16)$$

for each $m = 0, 1, \dots, P-1$; padded and in row-major order. We will call these the translation buffers. In order to achieve maximum performance, it is thus necessary to copy data from the swap buffers into the translation buffers and vice versa. This is unfortunate, but there seems no way around this rearranging of data in memory.

Here the benefit of the row-major format becomes obvious. One row from a swap buffer corresponds to exactly one row in the corresponding translation buffer. We can increase performance by choosing v such that one row corresponds to a fixed number of entire cache lines. For x86 systems with AVX support, this achieved by the choice $v = 8$ for double precision: one row of these matrices then exactly corresponds to 64 bytes, the size of a cache line. We can thus always copy entire cache lines at once instead of proceeding element-wise in a scalar, non-vectorised fashion.

3.4 Summary: The Entire Algorithm

We now have gathered all the main ingredients of the algorithm implemented in `solidfmm`, and are in a position to summarise it here. Thus, let there be ν solids $M[0], \dots, M[\nu - 1]$ and shift vectors $r_{AB}[0], \dots, r_{AB}[\nu - 1]$ be given. We then proceed as follows, where for brevity we will omit the indices $[0], [1], \dots, [\nu - 1]$ from now on:

- (1) For $n = 0, \dots, P$, and for each ν compute the following quantities: $|r_{AB}|^n, |r_{AB}|^{-n}, e^{in\alpha}, e^{in\beta}$. The exponential terms are powers of $e^{i\alpha} = \cos \alpha + i \sin \alpha, e^{i\beta} = \cos \beta + i \sin \beta$, where:

$$\begin{aligned} \cos \alpha &= \frac{y}{\sqrt{x^2 + y^2}}, & \cos \beta &= \frac{z}{|r_{AB}|}, \\ \sin \alpha &= \frac{x}{\sqrt{x^2 + y^2}}, & \sin \beta &= -\frac{\sqrt{x^2 + y^2}}{|r_{AB}|}. \end{aligned} \quad (17)$$

Thus, no trigonometric functions are necessary for this computation. Special care needs to be taken for α when $x = y = 0$. In this case: $\cos \alpha = 1$ and $\sin \alpha = 0$.

- (2) For each row $n = 0, \dots, P - 1$:
- Copy row n from all of the ν solids into the swap buffers.
 - Scale and rotate around z axis with angle α : $M_n^m \mapsto \frac{M_n^m}{|r_{AB}|^{m+1}} e^{im\alpha}, m = 0, 1, \dots, n$.
 - Swap x - and z -axes:

$$\Re(M_n^m) \mapsto \sum_{l=0}^n F_n^{m,l} \Re(M_n^l), \quad \Im(M_n^m) \mapsto \sum_{l=0}^n G_n^{m,l} \Im(M_n^l), \quad m = 0, 1, \dots, n. \quad (18)$$

Only every other entry in the matrices $F_n^{m,l}, G_n^{m,l}, l = 0, \dots, n$ is non-zero.

- Rotate around z axis by angle β : $M_n^m \mapsto M_n^m e^{im\beta}, m = 0, 1, \dots, n$. (No scaling)
 - Swap x - and z -axes again, according to (18).
 - Copy the result into the translation buffers.
- (3) For each column $m = 0, \dots, P - 1$: compute the matrix–matrix product (6), apply the signs $(-1)^{n+m}$.
- (4) For each row $n = 0, \dots, P - 1$:
- Gather row n for each of the ν solids from the translation buffers and store them into the swap buffer.
 - Swap the x - and z -axes:

$$\Re(L_n^m) \mapsto \sum_{l=0}^n F_n^{l,m} \Re(L_n^l), \quad \Im(L_n^m) \mapsto \sum_{l=0}^n G_n^{l,m} \Im(L_n^l), \quad m = 0, 1, \dots, n. \quad (19)$$

Here the transposed matrices $F_n^{l,m}, G_n^{l,m}$ are used.

- Rotate around z axis by the negative angle $-\beta$: $L_n^m \mapsto L_n^m e^{-im\beta}, m = 0, 1, \dots, n$. (No scaling.)
- Swap x - and z -axes again, according to equation (19).
- Rotate around z axis by $-\alpha$ and undo the scaling: $L_n^m \mapsto \frac{L_n^m}{|r_{AB}|^n} e^{-im\alpha}, m = 0, 1, \dots, n$. Note that the denominator has power n , not $n + 1$.
- Store the result at the desired output location.

4 PERFORMANCE MEASUREMENTS

At the moment, `solidfmm` comes in version 1.2 with generic microkernels and optimised kernels for AVX and AVX-512. We consider the timings for the M2L kernel only, as it is the most crucial of the FMM's translations. The benchmarks

can be carried out using the executables `benchmark_m2l` and `benchmark_m2l_naive` for the accelerated and naïve implementations, respectively. These programmes carry out a large number of M2L translations for each order $P = 1, \dots, 50$ and measure the time needed to complete the task. Afterwards this amount of time is divided by the number of translations. The naïve implementation uses simple, four-fold nested loops to implement the double height kernel (3).

We carried out experiments on a single core of an Intel Xeon W-10885M, which supports AVX, and an Intel Xeon Platinum 8160, supporting AVX-512. The results are illustrated in Figure 4. The naïve implementation shows the expected $O(P^4)$ complexity. `solidfmm`, on the other hand, performs faster than expected: we observe $O(P^2)$ or better for all relevant orders, in contrast to the asymptotic complexity of $O(P^3)$. We believe that this is due to the following effects. The microkernels only achieve a fraction of their peak performance when applied to small problems. Thus, the growing complexity is compensated by higher computational efficiency. At the largest orders we then finally begin to see an increased slope. For the AVX-512 version one can clearly observe the effects of the blocking scheme with $\mu = 14$: at order $P = 14$ the slope increases to about $O(P^2)$, another increase is visible at $P = 28$.

Already at $P = 10$ we observe a 33-fold speed up for the Xeon Platinum 8160, while for the W-10885M it is 28. These numbers keep on increasing, at $P = 20$ the respective speed ups are 124 and 94. We therefore believe that `solidfmm` is particularly interesting for high accuracy computations.

ACKNOWLEDGMENTS

This research was carried out under funding of the German Research Foundation (DFG), project ‘Vortex Methods for Incompressible Flows’, grant number 432219818. Without their support, this project would not have been possible.

I also received funding from the German National High Performance Computing (NHR) organisation.

I would also like to acknowledge the work of Simon Paepenmöller, one of my student workers. He helped in the development of preliminary software designs, and the tracking of many nasty sign bugs. This work is completely new, but draws from conclusions from these initial attempts and would not have been possible without them.

APPENDIX

Here, for completeness, we repeat the recurrence relations as given by Dehnen [3].

Regular and Singular Harmonics

Let $r = (x, y, z)^\top$ be given. Starting with $S_0^0(r) = |r|^{-1}$ and $R_0^0(r) = 1$, one continues with the diagonal:

$$S_n^n = (2n - 1) \frac{x + iy}{|r|^2} S_{n-1}^{n-1}, \quad R_n^n = \frac{x + iy}{2n} R_{n-1}^{n-1}, \quad (20)$$

and then obtains the remaining entries via:

$$\begin{aligned} |r|^2 S_n^m &= (2n - 1)z S_{n-1}^m - ((n - 1)^2 - m^2) S_{n-2}^m, \\ (n^2 - m^2) R_n^m &= (2n - 1)z R_{n-1}^m - |r|^2 R_{n-2}^m. \end{aligned} \quad (21)$$

The Matrices $B_n^{m,l}$

Starting with $B_0^{0,0} = 1$, one has:

$$2B_{n+1}^{m,l} = B_n^{m,l-1} - B_n^{m,l+1}, \quad 2B_{n+1}^{m,\pm 1,l} = B_n^{m,l-1} \pm 2B_n^{m,l} + B_n^{m,l+1}, \quad (22)$$

where it is implicitly assumed that $B_n^{m,l} = 0$, whenever $|l| > n$.

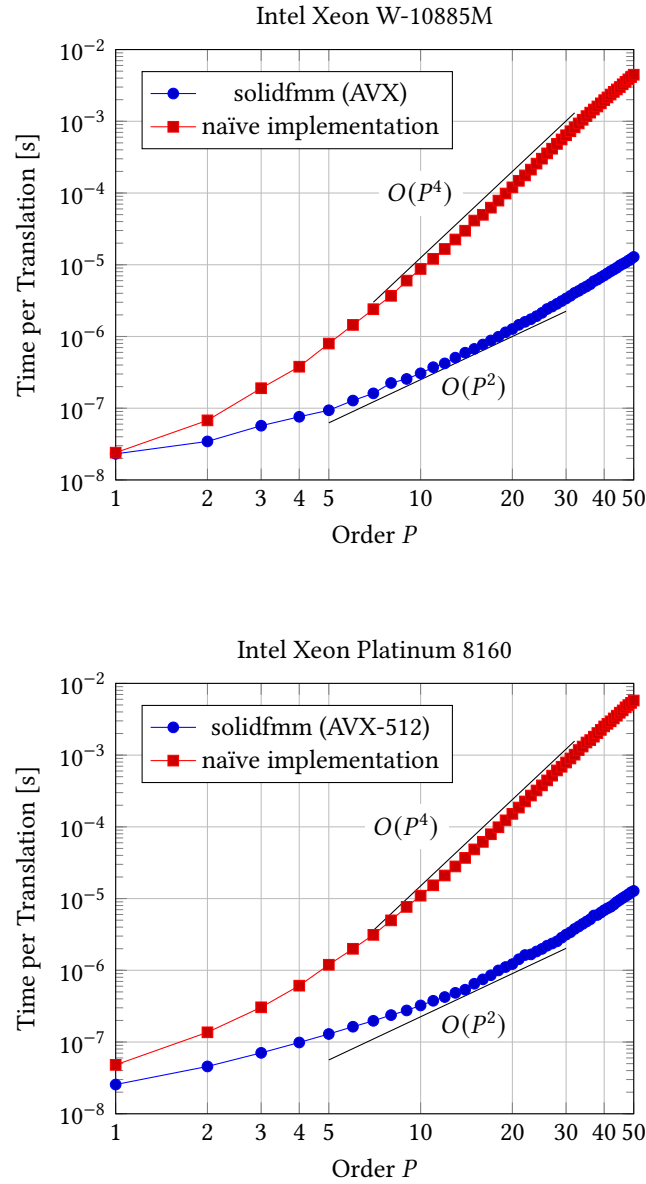


Fig. 4. Timings for performing a single M2L translation of order P , for a naïve, loop-based implementation and `solidfmm` using double precision arithmetic, performed on a single core of an Intel Xeon W-10885M (top) and an Intel Xeon Platinum 8160 (bottom). The timings were obtained by carrying out a large number of M2L translations, the total time was then divided by this number. `solidfmm` is vectorised using respectively AVX and AVX-512 with $\nu = 8$ and $\nu = 16$, the naïve implementation is scalar and uses a simple, four-fold nested loop to implement the double height kernel (3). One clearly sees the $O(P^4)$ complexity of the naïve code. `solidfmm`, on the other hand, shows an empirical complexity of $O(P^2)$ or better for the practically relevant orders, clearly outperforming the asymptotic bound of $O(P^3)$. For the AVX-512 version, the effect of the blocking scheme ($\mu = 14$) becomes apparent at orders $P = 14$ and $P = 28$, where the slope starts to slightly increase.

REFERENCES

- [1] Barry A. Cipra. 2000. The Best of the 20th Century: Editors Name Top 10 Algorithms. *SIAM News* 33, 4 (May 2000).
- [2] Olivier Coulaud, Pierre Fortin, and Jean Roman. 2008. High performance BLAS formulation of the multipole-to-local operator in the fast multipole method. *J. Comput. Phys.* 227, 3 (Jan. 2008), 1836–1862. <https://doi.org/10.1016/j.jcp.2007.09.027>
- [3] Walter Dehnen. 2014. A fast multipole method for stellar dynamics. *Computational Astrophysics and Cosmology* 1, 1 (2014), 1–23. <https://doi.org/10.1186/s40668-014-0001-7>
- [4] William D. Elliott and John A. Board, Jr. 1996. Fast Fourier Transform Accelerated Fast Multipole Algorithm. *SIAM Journal on Scientific Computing* 17, 2 (March 1996), 398–415. <https://doi.org/10.1137/S1064827594264259>
- [5] Leslie F. Greengard and Vladimir Rokhlin. 1987. A fast algorithm for particle simulations. *J. Comput. Phys.* 73, 2 (Dec. 1987), 325–348. [https://doi.org/10.1016/0021-9991\(87\)90140-9](https://doi.org/10.1016/0021-9991(87)90140-9)
- [6] Leslie F. Greengard and Vladimir Rokhlin. 1997. A new version of the Fast Multipole Method for the Laplace equation in three dimensions. *Acta Numerica* 6 (Jan. 1997), 229–269. <https://doi.org/10.1017/S0962492900002725>
- [7] Robert A. van de Geijn, Margaret Myers, and Devangi Parikh. 2021. *LAFF-On Programming for High Performance*. ulaff.net. <https://www.cs.utexas.edu/users/flame/laff/pfhp/>
- [8] Field G. van Zee and Robert A. van de Geijn. 2015. BLIS: A Framework for Rapidly Instantiating BLAS Functionality. *ACM Trans. Math. Software* 41, 3 (June 2015), 1–33. <https://doi.org/10.1145/2764454>
- [9] H. Y. Wang and R. LeSar. 1996. An efficient fast-multipole algorithm based on an expansion in the solid harmonics. *The Journal of Chemical Physics* 104, 11 (March 1996), 4173–4179.
- [10] Christopher A. White and Martin Head-Gordon. 1996. Rotating around the quartic angular momentum barrier in fast multipole method calculations. *Journal of Chemical Physics* 105, 12 (Sept. 1996), 5061–5067. <https://doi.org/10.1063/1.472369>
- [11] Ryo Yokota. 2013. An FMM Based on Dual Tree Traversal for Many-Core Architectures. *Journal of Algorithms & Computational Technology* 7, 3 (Sept. 2013), 301–324. <https://doi.org/10.1260/1748-3018.7.3.301>